International Journal of Civil Engineering

Geotechnique

Mechanics of projectile penetration into non-cohesive soil targets

M. Anwer Khan[1,*]

Received: September 2014, Accepted: January 2015

Abstract

Investigation of projectiles penetration phenomenon has been carried out in non-cohesive soil (Sand) targets under dry, saturated and compacted conditions. Analytical studies have been performed on the linear and non-linear soil models to obtain penetration depth formulae for ogival nose projectile and the results are verified by experimental studies. In present work, three ogival nose projectiles each having weight of 1.0 kg and nose angle of 15^o, 30^o and 45^o are dropped from a height of 10.0 m in rectangular tank filled up by non-cohesive soil target. The rigid projectiles made an impact on a uniform target material at normal incidence with striking velocity of 14 m/s and proceeded to penetrate at rigid-body velocity. The models require geometrical parameters of the projectile types, velocity and target shear strength for the overall penetration depth of projectile. In addition, some parametric studies have been also carried out for academic and field interest.

Keywords: *Projectile penetration, Projectile, Non-cohesive soil target, Caliber radius head.*

1. Introduction

After the end of Second World War most of the countries began to make shelter against nuclear attack. The recent nuclear tests conducted in the subcontinent have further awakened the investigators for undertaking extensive study on the subject of projectile/missile impact upon different type of targets, particularly the geo-materials under which the strategic structures such as army bunkers and Nuclear Power Plants (NPP) may be buried. Burying of these strategic structures is considered to be the most effective and efficient way to save them from any possible damage. The safety or destruction of these structures requires the correct estimation of penetration depth in overlying geo-material and forces exerted by missiles (with no explosive) on these structures.

Soil penetration by projectiles has motivated many generations of researchers. Historically, studies in missile penetrations were initiated according to military needs more than two centuries ago [1,2]. Some early studies by Allen [3], Thompson [4] and Zukas et al. [5] have focused on the impact and subsequent penetration of instrumented projectiles. Experimental studies on the dynamics of soil penetration by low-velocity projectiles stimulated the development of theoretical modeling of the dynamic phenomena of impact and penetration in solids [5] and in soils [6].

These theories were mostly based on dynamic plasticity and dynamic wave propagation and did not adequately characterize the extremely complex process of vertical penetration in granular soils.

Current experimental studies have concentrated on assessment of the influence of projectile shape on depth of penetration [7,8,9] and fitting of results to existing theoretical models [10,11]. Such an approach avoids analysis of the physical properties/processes of penetration phenomena. Comparison of theoretical and experimental results allowed us to solve the inverse problem of dynamic penetration and to determine the properties of penetrated soil media. Seguin et al. [12] developed a model for the penetration of the projectile in the granular bed including a friction law between the projectile and the grains, a viscous dissipation in the bed and a force from the collisions between the projectile and the granular material. The model suggests that the penetration depth is a power law of the total drop distance.

A detailed review of past investigators shows that considerable work has been done in the area of impact of missiles on plates, shells etc. [13,14]. However, studies available on impact of missiles on geo-material targets are scanty. The past investigators have carried out penetration study of missiles into geological targets using three types of models: (a) *Empirical Model* (b) *Cavity Expansion Model* and (c) *Model of Orthogonal Layers.* Empirical models are specific to the experimental data for which they have been developed. The Cavity Expansion model has been developed with the assumptions that when a missile impacts penetrates the geo-material target, it creates a cavity. This cavity expands under the action of stress waves generated into the target medium. To study the shape of cavity thus formed and its expansion phenomenon, *Spherical* and *Cylindrical Cavity Expansion Model* theories have been proposed by Norwood and Sears

** Corresponding author: mehboobcivil@yahoo.co.in*
1 Associate Professor, Department of Civil Engineering, Aligarh Muslim University, Aligarh, -202 002, (U. P) India

[15]. *Model of orthogonal layers* has been developed by Yankelevisky [16] as an attempt to advance the cavity expansion approach towards a better physical representation of soil-penetrator interaction and obtained more useful results, which are an improvement over the previous models. In these models, soil medium is considered as a set of independent layers and the element line is assumed orthogonal to the nose surface.

Using above models, past investigators have proposed various formulae for the prediction of deceleration-time history, penetration depth, forces at missile nose etc. These expressions have been mostly derived for linear material model of the target and normal impact of missiles having or assuming equivalent conical nose shape. The friction on nose and missile aft body has been neglected by most of the past investigators. In addition to these, almost all the investigators have carried out their analyses on deterministic basis [15,16]. However, most of the parameters such as material characteristics, angle of impact, velocity of missile and occurrence of various events are highly probabilistic. Mechanics of missile penetration requires proper modeling of target material, which is still considered the weakest link in the chain of analyses. However, many models have been recently developed by Yu and Mictchell [17] and Danziger et al. [18] for modeling of geological targets, but none of the models are capable enough to simulate the response of missile penetration properly. It is proposed, therefore to improve the material models.

2. Experimental Studies of Projectile Penetration in Non-Cohesive Soil Targets

An experimental study of projectile penetration into non-cohesive soil (sand) target was performed on the three projectiles of ogival nose shapes (O_1, O_2 and O_3) having nose angles of 15°, 30° and 45°. The projectiles were made of mild steel and having weight, diameter and length of shank (l) equal to 1 kg, 40 mm and 210 mm respectively (Fig. 1). The geometrical data of three ogival nose projectiles are shown in Table 1. The weight of projectiles was made same by keeping some hollow portion inside the projectile where as the nose length of projectiles was dependent on their nose angle or Caliber Radius Head (CRH). The caliber radius head of ogival nose, ψ is given by $\psi = \frac{r}{2R}$ where, R is the radius of aft body and r is the radius of curvature of ogival nose given by: $r = \frac{R}{2}\left\{1+\left(\frac{L}{R}\right)^2\right\}$ where, L is nose length of projectile (Fig. 5).

Fig. 1 Ogival nose projectiles with nose angles of 15°, 30° and 45°

Table 1 Geometrical data of projectiles*

Projectile	Mark	Weight (kg)	Nose angle θ (deg.)	Nose length L (mm)	Total length L' = L+*l (mm)	$\frac{L'}{2R}$	Caliber radius head (CRH) ψ
Ogival nose	O_1	1.000	15**	151.9	361.9	9.05	14.65
	O_2	1.000	30**	74.6	284.6	7.12	3.72
	O_3	1.000	45**	48.3	258.3	6.46	1.70

* l = shank length, R = radius of shank (= 20 mm), ** Equivalent nose angle

All the projectiles were dropped from a constant height of 10.0 m with a striking velocity of 14.0 m/s into rectangular wooden tank filled with non-cohesive target materials under different conditions of moisture and degree of compaction. The experimental tank was rectangular in plan with the inside dimensions of 1.50 m × 0.75 m × 0.75 m (high). The three vertical sides and base of the tank were made of ¾ inch plywood and aluminum sheet of 3 mm thickness was affixed to the wood on the inside face of the tank. For observations of projectile penetration, a transparent glass sheet was fixed in the fourth vertical face of the tank (Fig. 2).

Fig. 2 Rectangular tank filled up by non-cohesive target material

The physical properties of non-cohesive target material were determined in geotechnical engineering laboratory by conducting experimental tests according to IS specification (Table 2). A quantitative determination of the particle size distribution was made by sieve analysis with a set of IS sieves in micron (600 μ, 425 μ, 300 μ, 212 μ, 150 μ and 75 μ). The particle size distribution curve of sand is shown in Fig. 3. The Standard Proctor Compaction Test (AASHO Test)-IS: 2720-VII, determined the optimum moisture content (OMC) and maximum dry density, γ_{dmax} (Fig. 4). The shear strength parameters of sand were determined by performing consolidated drained triaxial tests with confining pressures of 50 kN/m^2, 100 kN/m^2 and 150 kN/m^2. The oven-dried sand was sieved through IS: 600 μ sieve and filled in the rectangular tank in loose state by free fall from a fixed height of 150 mm, for the saturated sand deposit, the tank was pounded with water so as to fill the voids for complete saturation and the compacted sand target was deposited at OMC in three equal layers, each layer tamped by giving 100 number of blows with a 4.6 kg hammer having loaded area of 150 mm × 150 mm and free fall of 300 mm. The required 100 number of blows corresponding to maximum dry density was obtained by trial method.

Table 2 Physical properties of non-cohesive soil targets

Optimum moisture content (OMC)	12.30 %
Maximum dry density (γ_{dmax})	15.00 kN/m^3
Proctor density of sand compacted at OMC (γ)	16.85 kN/m^3
Void ratio of sand compacted at OMC, e = e_{min}	77.21 %
Porosity (n)	44.16 %
Shear strength at OMC from triaxial test (τ_o)	128.20 kN/m^2
Maximum shear strength at OMC (τ_m)	256.30 kN/m^2
Specific gravity by Pycnometer (G)	2.66
Coarse fraction (> 2 mm)	0.00 %
Medium fraction (75 μ to 425 μ)	94.11 %
Fine fraction (< 75 μ)	4.13 %
Uniformity coefficient, $C_u = D_{60}/D_{10}$	01.82
Coefficient of curvature, $C_c = (D_{30})^2 / D_{60}\, D_{10}$	1.12
Effective size (D_{10})	0.14 mm
Soil classification as per IS: 1498-1970	Uniformly graded
Fineness modulus (FM)	1.62
Unit weight in dry state (γ_d)	13.50 kN/m^3
Unit cohesion (c)	0.00 kN/m^2
Angle of internal friction (ϕ)	32.50^o
Unit weight in saturated state (γ_{sat})	17.80 kN/m^3
Unit apparent cohesion in saturated sate (c_m)	0.52 kN/m^2
Angle of internal friction in saturated state (ϕ_m)	20.60^o

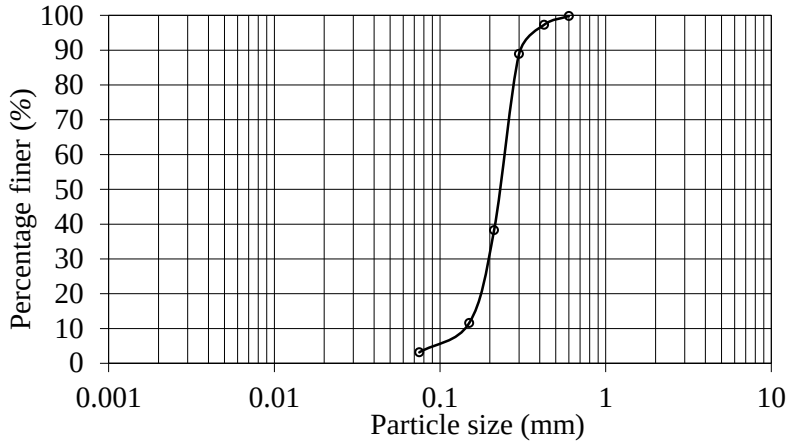

Fig. 3 Grain size analysis of non-cohesive soil target

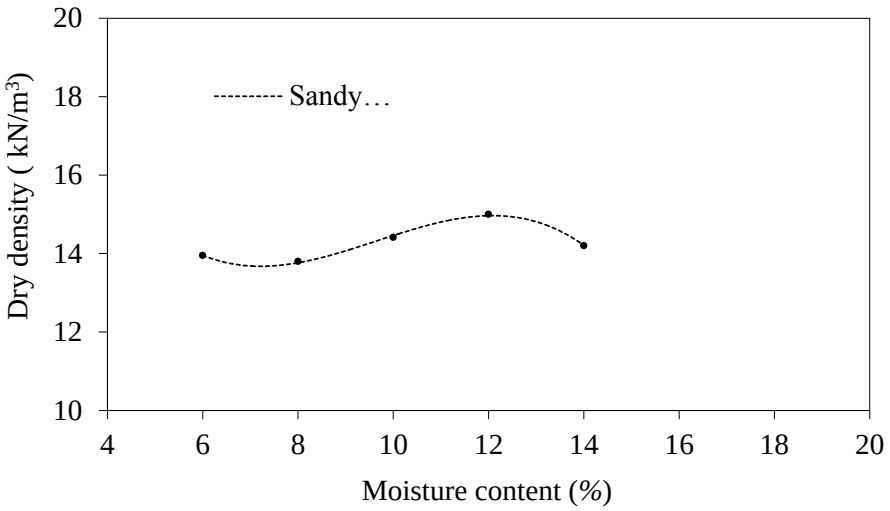

Fig. 4 Compaction curve of non-cohesive soil target

3. Methodology of Projectile Penetration in Non-Cohesive Soil Targets

The target points of projectile in experimental tank are first aligned by hanging a plumb bob from 10.0m high building and then the projectiles are dropped freely under the action of gravity. Thus, the striking velocity of each projectile was 14.0 m/s. The distance between the target striking points of the projectiles were selected in such a way that the effect of experimental tank walls and overlapping of stress zones due to the penetration of projectiles could be avoided. The number of projectiles penetrated into a target was not more than three. Those tests in which the strike of the projectile was not normal were discarded and were repeated in the next round for experimental tank.

The depth of penetration of projectiles was measured accurately with a precision of 1 mm with the help of scale. Each test was repeated thrice with altered sequence of strike and the average value of the depth of penetration was recorded. The recorded values of the depth of penetration of three ogival nose shape projectiles into non-cohesive soil targets in tank is given in Table 4. The cored samples from non-cohesive soil targets were tested in the laboratory for determining the basic properties of soil *viz*. bulk density, dry density, moisture content and shear strength parameters (unit cohesion, *c* and angle of internal friction, *ø*). The shear strength parameters were determined by triaxial test.

4. Problem Formulation

The problem has been formulated under the following assumptions

- The missile is rigid i.e. deformation of missile is negligible and only soil deformation has been considered.
- Impact of missile is normal and axi-symmetric.
- Wave propagation is one dimensional and in the radial direction.
- The missile does not carry any warhead and no explosion has been considered.
- The loss of energy in the form of heat and sound has been neglected.

4.1. Material model

The target medium is described by a linear hydrostat, assuming a linear shear failure stress and pressure relation as given below. Many soil materials with low water content can be modeled with these idealizations [8].

$$\eta^* = \left(1 - \frac{\rho_0}{\rho^*}\right) \tag{1}$$

In the present study following Mohr-Coulomb yield criterion has been considered which may be expressed as

$$\sigma_r - \sigma_\theta = \tau_0 + \lambda\, p \tag{2}$$

where, $\lambda = \lambda_1$ for linear material model and $\lambda = \lambda_1 + \lambda_2 p$ for non-linear material model. Here, τ_o, λ_1 and λ_2 are the parameters which have to be obtained from best fit of experimental data plotted between shear strength and hydrostatic pressure.

$$\mathrm{p} = (\sigma_r + 2\sigma_\theta)/3 \tag{3}$$

The eq. (3) has been obtained assuming the vertical stress σ_z to be equal to the circumferential stress σ_θ during the penetration event.

where,

η^* = locked volumetric strain; ρ_0 = initial mass density; ρ^* = locked mass density; σ_r, σ_θ = radial and tangential components of Cauchy stress (positive in compression); τ_0 , λ = define the yield condition; and p = hydrostatic pressure.

4.2. Stresses in the soil medium

When a rigid missile nose penetrates a uniform target medium with normal incidence, a spherically symmetric cavity is formed. This spherically symmetric cavity expands with constant velocity *V* under the action of stress waves. This expansion produces plastic and elastic response regions bounded by the radii *Vt* and *ct*, where *t* is the time and *c* is elastic-plastic interface velocity. The element of such an expanded layer at a radial distance *r* from the axis of symmetry is subjected to shear stress $(\sigma_r - \sigma_\theta)$ and hydrostatic pressure *p* given by eq. (2) and eq. (3). Now using above material model, following equations of momentum and mass conservation in Langrangian coordinates have been derived [8].

$$(r+u)^2 \frac{\partial \sigma_r}{\partial r} + 2\left(1+\frac{\partial u}{\partial r}\right)(r+u)(\sigma_r - \sigma_\theta) + \rho_o r^2 \frac{\partial^2 u}{\partial t^2} = 0 \tag{4}$$

$$\frac{1}{3}\frac{\partial}{\partial r}\left[(r+u)^3\right] = \frac{\rho_o}{\rho} r^2 \tag{5}$$

Where, *r* is the Lagrangian coordinate ρ is the current density and u is the radial displacement (positive outward) which satisfies the following boundary condition at the cavity interface:

$$u(r=0,t) = Vt \tag{6}$$

To reduce eq. (4) and eq. (5) into ordinary differential equations following similarity transformations may be used:

$$\xi = \frac{r}{ct} \tag{7}$$

$$\bar{u}(\xi) = \frac{u(r,t)}{ct} \tag{8}$$

$$S = \frac{\sigma_r}{\tau_o} \tag{9}$$

Substituting above transformations into eq. (4) and eq. (5), we get

$$(\xi+\bar{u})\frac{dS}{d\xi} + 2\alpha \frac{d}{d\xi}(\xi+\bar{u})S = \frac{-2\alpha}{\lambda}\frac{d}{d\xi}(\xi+\bar{u}) - \frac{\rho_0 c^2}{\tau_0}\frac{\xi^4}{(\xi+\bar{u})}\frac{d^2\bar{u}}{d\xi^2} \tag{10}$$

$$\frac{1}{3}\frac{d}{d\xi}\left[(\xi+\bar{u})^3\right] = (1-\eta^*)\xi^2 \tag{11}$$

where, $\alpha = 3\lambda/(3+2\lambda)$ (12)

The solution of above differential equations for $\xi = 0$ may be expressed as

$$S(\xi=0) = A + B\rho_o V^2/\tau_o \tag{13}$$

where,

$$A = \frac{1}{\alpha}\left(\frac{1+\tau_o/2E}{\gamma}\right)^{2\alpha} - \frac{1}{\lambda} \tag{14}$$

$$B = \frac{3}{(1-\eta^*)(1-2\alpha)(2-\alpha)} + \frac{1}{\gamma^2}\left(\frac{1+\tau_o/2E}{\gamma}\right)^{2\alpha} \left\{ \begin{array}{l} (3\tau_o/E) + \eta^*(1-3\tau/2E)^2 \\ -\dfrac{\gamma^3[2(1-\eta^*)(2-\alpha)+3\gamma^3]}{(1-\eta^*)(1-2\alpha)(2-\alpha)(1+\tau_o/2E)^4} \end{array} \right\} \tag{15}$$

The above equation is indeterminate for $\lambda = 0$ and $\lambda = 3/4$. These cases therefore separately analyzed and following equations for A and B has been obtained

For $\lambda = 0$

$$A = \frac{2}{3}\left\{1 - \ln\left[\frac{(1+\tau_o/2E)^3 - (1-\eta^*)}{(1+\tau_o/2E)^3}\right]\right\} \tag{16}$$

$$B = \frac{3}{2(1-\eta^*)} + \frac{(3\tau_o/E) + \eta^*(1-3\tau_o/2E)^2}{\left[(1+\tau_o/2E)^3 - (1-\eta^*)\right]^{2/3}} - \frac{\left[(1+\tau_o/2E)^3 - (1-\eta^*)\right]^{1/3}}{2(1+\tau_o/2E)^4}\left[1 + \frac{3(1+\tau_o/2E)^3}{(1-\eta^*)}\right] \tag{17}$$

For $\lambda = 3/4$

$$A = 2(1+\tau_o/2E)/\gamma - 4/3 \tag{19}$$

$$B = \frac{-2\ln\gamma}{(1-\eta^*)} + \frac{(1+\tau_o/2E)[3\tau_o/E + \eta^*((1-3\tau_o/2E)^2]}{\gamma^3} - \frac{2}{3}\left[\frac{1}{(1+\tau_o/2E)^3} - \frac{3\ln(1+\tau_o/2E)}{(1-\eta^*)}\right]$$

The cavity expansion velocity V may be obtained in terms of missile rigid body velocity V_z, nose length L, penetration depth z, radius of aft body R and CRH ψ as [19]

$$V = V_Z \frac{(L-z)}{2R\psi} \tag{20}$$

Having known the *S* at ξ = 0 from eq. (13), we can estimate the radial stress component σ_r at the missile nose using eq. (9).

4.3. Forces on missile nose and deceleration

The penetration of missile into the target results in the radial movement of the target material at the cavity interface which produces radial stress in the target material. The incremental radial force on the missile nose for a thin target thickness *dz* is given by

$$dF_r = 2\pi\sigma_r(0)R(z)dz \tag{21}$$

Where, σ_r *(0)* is the radial stress in the target material at the cavity expansion and *R (z)* is the radius of the missile nose at a distance *z* from its tip (Fig. 5). The expression of *R (z)* for an ogive nose is given by (Siddiqui and Abbas 2002):

$$R(z) = -a + \sqrt{a^2 - z^2 + 2Lz} \tag{22}$$

where, $a = (R'-R)$; R' = radius of the ogive nose; R = radius of the aft body of missile; and L = nose length of missile.

The vertical force at the nose of the missile due to the vertical stiffness of the target material of thickness *dz* is given by

$$dF_v = dF_r \tan\theta \tag{23}$$

Where,

dF_v = incremental vertical force; dF_r = incremental force in radial direction and θ = equivalent cone angle.

Force acting at the nose is the drag force which is tangential to the surface of the missile nose arising due to the friction between the target material and missile. The drag force has not been considered by Forrestal et al. [20] in their penetration analysis. The magnitude of incremental drag force dF_d for the elemental target thickness *dz* is equal to the product of coefficient of dynamic friction between the missile surface and the target material (μ_d) and force normal to the missile nose (dF_n) i.e.

$$dF_d = \mu_d dF_n \tag{24}$$

where, $dF_n = dF_r \sec\theta$, therefore,

$$dF_d = \mu_d dF_r \sec\theta \tag{25}$$

Hence, the total incremental *vertical upward component* (dF_z) of the target reaction will be

$$dF_z = dF_v + dF_d\cos\theta = dF_r\tan\theta + \mu_d\, dF_n\cos\theta = dF_r(\mu_d + \tan\theta) \tag{26}$$

where, the radial force dF_r and vertical force dF_v are in fact the radial and vertical components of the normal force dF_n. The total upward vertical target reaction on the missile nose has been obtained by integrating eq. (22) from 0 to penetration depth *z* (where, z ≤ L)

$$F_z = \int_0^z (\mu_d + \tan\theta)dF_r$$

$$= \int_0^z (\mu_d + \tan\theta)2\pi\sigma_r R(z)dz \tag{27}$$

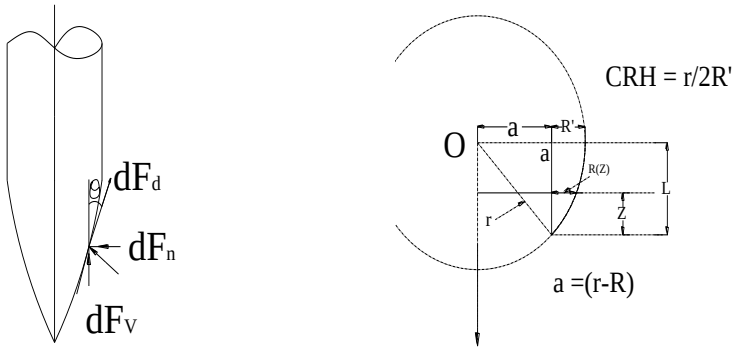

Fig. 5 Drag force acting tangentially to the surface of the missile nose

If the depth of penetration of missile is greater than the nose length then the upper limit of integration will be up to *L* because we are getting reaction only on the nose. The equation eq. (27) has been applied for the estimation of total vertical target reaction F_z

for ogive nose shaped missiles. The force F_z will be given as

$$F_z = \int_0^z (\mu_d + \tan\theta)2\pi\sigma_r R(z)dz \tag{28}$$

The substitution of *R (z)* for ogive nose from eq. (22) and the value of tanθ at a distance *z* from the tip of the nose in eq. (28), lead to

$$F_z = 2\pi \int_0^z \sigma_r R(z)\left(\frac{L-z}{R(z)+a}+\mu_d\right)dz$$
$$= 2\pi \int_0^z \sigma_r \left(-a+\sqrt{a^2-z^2+2Lz}\right) \quad (29)$$
$$\left(\frac{L-z}{\sqrt{a^2-z^2+2Lz}}+\mu_d\right)dz$$

It is to be noted here that σ_r for ogive nose is a function of *z*. The force F_z given by eq. (29) for the ogive nose can be integrated using any standard numerical integration scheme.

4.40 Response estimation

To obtain the response time histories of velocity, penetration depth, and the deceleration of missile, the dynamic equilibrium of missile has been considered that results in the following well known equation:

$$m\frac{dV_z}{dt} = -F_z \quad (30)$$

The integration of above equation, using any standard numerical integration scheme, will yield time histories of velocity, penetration depth and the deceleration of missile. In the present study, the forward finite difference approach has been employed for its integration. Using this approach, the velocity V_z, deceleration a_z and the penetration depth *z* of missile at (i+1) th time step can be obtained by the following relations:

$$V_z^{i+1} = V_z^i - \frac{1}{m}(F_z^{i+1}\Delta t) \quad (31)$$

$$a_z^{i+1} = \frac{V_z^{i+1}-V_z^i}{\Delta t} \quad (32)$$

$$z^{i+1} = z^i + V_z^i \Delta t \quad (33)$$

5. Numerical Studies

The methodology for the penetration analysis of soil targets under projectile impact has been validated. The test results of experimental study of projectile penetration in non-cohesive soil (sand) under different conditions of moisture and compaction have been presented. The tests conducted for the study being of low velocity, some published results involving high velocity of strike have been used for the purpose of validation of the models. The parameters considered for the purpose of validation are depth of penetration, deceleration-time history, forces at the projectile nose, stresses in the target material and its variation with depth and radial distance. The results of analysis of published work available in literature have been compared with the results of present study. Some useful parametric studies have also been performed in the present study to obtain the results of practical interest.

5.1. Validation of model with present experiment

The spherical cavity expansion (SCE) model developed for the penetration analysis of soil target have been validated with the help of the experiments carried out in the laboratory for low velocity of strike. Whereas, the experiments available in literature have been used for the purpose of validation of model for higher velocity of strike. The experimental data available for validation of the model is depth of penetration. Three projectile models of ogival nose shape with nose angle of 15^o, 30^o and 45^o, each having weight of 1.0 kg, used for penetration studies in non-cohesive soil targets for numerical modeling and experimental studies. The results obtained from experiments of penetration depths of the projectiles falling freely from a height of 10.0 m with striking velocity of 14 m/s into targets have been compared with the Forrestal and Luk Model [8] and model proposed in this study.

The target types employed in this study include, dry, saturated and compacted sandy soil target. The physical properties of sandy soil targets are given Table 1. To describe the soil material model completely, we need three important parameters τ_o, λ_1 and λ_2 (eq. (2)). These two parameters have been obtained by plotting the data on shear strength and hydrostatic pressure graph and then fitting linear and nonlinear curves to these data points (Fig. 6). We get following values of λ_1 and λ_2 for linear and nonlinear materials (Forrestal and Luk model [8]):

τ_o = 10.0 MPa ; λ_1 = 0.0 for linear model.

τ_o = 8.083 MPa ; λ_1= 0.091 and λ_2= -0.001 for nonlinear material model.

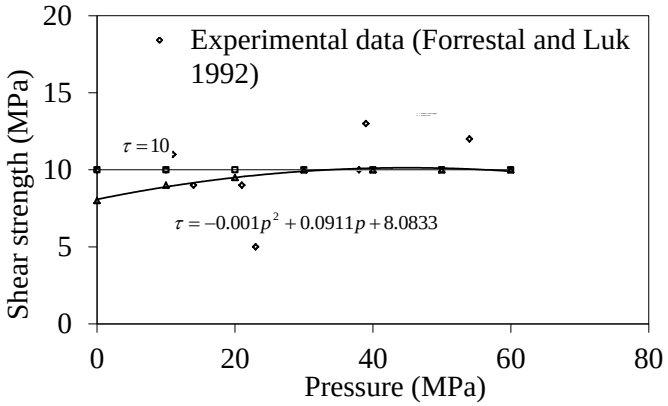

Fig. 6 Shear strength vs hydrostatic pressure for non-cohesive soil target

6. Results and Discussion

6.1. Non–Cohesive Targets

The three different categories of non-cohesive soil (sand) targets are considered in the present study,

a) Dry sand b) Saturated sand c) Compacted sand at OMC.

6.1a. Dry sand

It is observed from Table 3 that the penetration depths of ogival nose projectiles (O1, O2 and O3) predicted by Forrestal and Luk model are 35 % to 40.8 % less than the experimental values. Whereas, the penetration depth of projectiles predicted by the proposed model for same nose types are only 6.5 % to 11.6 % less. Thus, it can be seen that the error in the prediction depth got much reduced in the proposed model as compared to the Forrestal and Luk model.

Table 3 Comparison of penetration depth of projectiles in loose and dry sand

S. No.	Nose shape	Experimental penetration depth (*mm*)	Predicted penetration depth (*mm*)			
			Forrestal Luk model	Error (%)	Proposed model	Error (%)
1.	O_1	554	330	**-40.4**	490	**-11.6**
2.	O_2	515	325	-36.9	465	-9.7
3.	O_3	460	295	-35.8	430	-6.5

6.1b. Saturated sand

For the saturated sand target, the predicted penetration depth by Forrestal and Luk model is 21.1 % to 24.8 % less than the experimental value. Whereas, the penetration depths of projectiles are 0.3 % to 1.3% less to the proposed model. Thus it is seen that the error in the prediction depth got reduced in the proposed model as compared to the Forrestal and Luk model (Table 4).

Table 4 Comparison of penetration depth of projectiles in saturated sand

S. No.	Nose shape	Experimental penetration depth (*mm*)	Predicted penetration depth (mm)			
			Forrestal Luk model	Error (%)	Proposed model	Error (%)
1.	O_1	254	191	**-24.8**	255	**-0.3**
2.	O_2	243	188	-22.7	242	-0.4
3.	O_3	224	179	-20.1	221	-1.3

6.1c Compacted Sand

The penetration depth predicted by proposed model is 0.5 % to 2.9 % less than the experimental value. Whereas, the penetration depth of projectiles predicted by Forrestal and Luk model is 13.2 % to 24.4 % less. Thus it is seen that the error in the prediction depth by proposed model is almost negligible and there is an improvement in the Forrestal and Luk model (Table 5).

Table 5 Comparison of penetration depth of projectiles in compacted sand

S. No.	Nose Shape	Experimental penetration depth (mm)	Predicted penetration depth (*mm*)			
			Forrestal and Luk model	Error (%)	Proposed model	Error (%)
1.	O_1	213	161	**-24.4**	212	-0.5
2.	O_2	158	125	-20.8	149	-5.7
3.	O_3	136	118	**-13.2**	132	-2.9

6.2. Comparison of Present Study Model with Forrestal and Luk Prediction

Table 6 shows that if friction force on missile nose is neglected, the prediction of Forrestal and Luk [8] is close to the experimental depth of penetration, however, if friction is considered; their prediction underestimates the depth of penetration. But the sliding friction on the nose of the projectile cannot be ignored in the present problem. Moreover, in the present study, though the depth of penetration neglecting friction is quite high but the consideration of friction gives the magnitude which is reasonably close to the actual depth of penetration particularly when nonlinear material model has been considered (difference is about 5%).

Table 6 Comparison of penetration depths

Model	Penetration depth (m)	
	Friction neglected	Friction considered
Forrestal and Luk (1992)	4.98	3.16
Present study (Linear)	6.23	4.34
Present study (Non-linear)	7.24	5.08
Average experimental value	-	5.04

It has been also observed that the nonlinear material model predictions are much better than corresponding linear material model prediction. This shows that the present study is a good improvement of Forrestal and Luk model [8].

6.3. Impact Velocity and Penetration Depth with Time

Fig. 7 shows that for striking velocity of 14 m/s of ogival nose projectile model, the penetration depth increasing and striking velocity reducing with time for present study and Forrestal and Luk models. This is an expected trend. Impact velocity is the measure of impact energy as the projectile penetrates into the soil the, impact velocity decreases and penetration depth increases with time. It has been also observed that the variation of velocity with time up to penetration of nose length is linear for Forestall and Luk model but it is non-linear for present study model. The penetration depth by present study model was obtained 30 % more than the Forrestal and Luk model. The reason for this pattern is that the analysis of Forrestal and Luk [8] considered the effect of projectile after full penetration of nose length but in the present study, the effect of projectile nose and shaft both are considered.

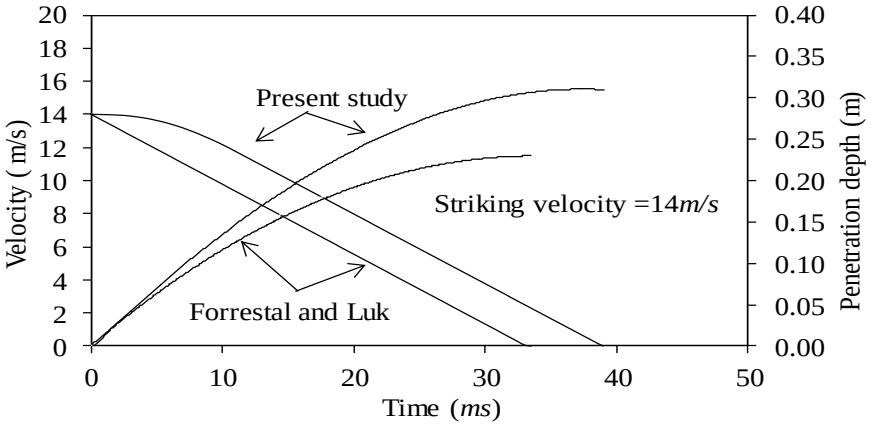

Fig. 7 Variation of velocity and penetration depth of projectile with time

6.4. Parametric Studies

To obtain the results of academic and field interest some parametric studies have been carried out, which are presented in subsequent subsections. The effect of a parameter on the penetration has been studied by varying the selected parameter and keeping all other parameters is fixed.

6.4.1. Effect of CRH

The variation of depth of penetration for different CRH values by keeping all other parameters fixed is shown in (Fig. 8). These figures show that the depth of penetration increases whereas deceleration decreases with the increase in the value of CRH of missile nose. It is due to the fact as *CRH* increases, the nose length increases (nose length = 252 mm, 294 mm and 331 mm for CRH = 3, 4, and 5 respectively) and shape of the nose becomes more pointed that makes the penetration easier and, therefore, penetration depth increases whereas deceleration decreases. This pattern is same for the linear as well as the nonlinear material models. However, since nonlinear material offers lesser resistance as compared to linear material, the missile of same CRH in the non-linear material stops at greater depth than the linear soil material.

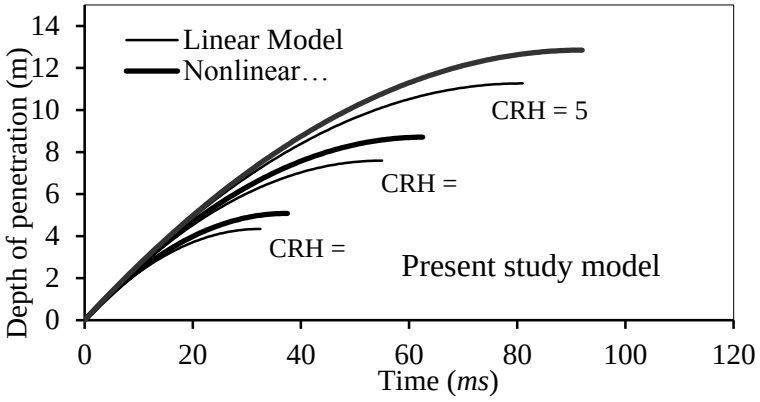

Fig. 8 Effect of CRH on penetration depth

6.4.2. Effect of coefficient of friction

The coefficient of friction is an uncertain parameter that directly governs the force of resistance offered by the material to the penetration of missile. It is expected that as the coefficient of friction increases, the depth of penetration should decrease. Fig. 9 shows the same trend and the variation is almost linear for practical purposes. For same value of coefficient of friction (0.13), the predicted value of penetration depth by present study nonlinear model was 17 % more than the linear model. The decrease of 10 % in value of coefficient of friction results an increase in penetration depth of 6.5 % for linear and non- linear models. For the same coefficient of friction, nonlinear model offers lesser resistance, results a greater penetration depth.

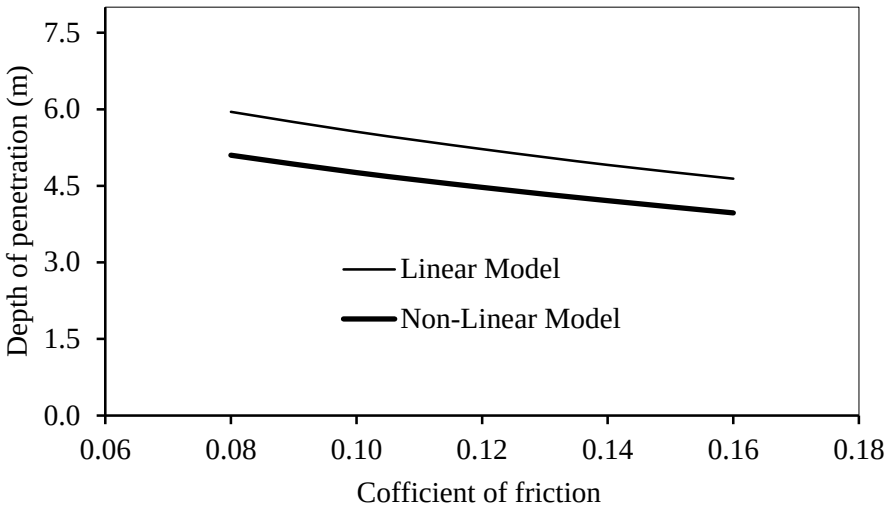

Fig. 9 Effect of coefficient of friction on penetration depth

6.4.3. Effect of mass

For given velocity, mass is directly proportional to the kinetic energy of missile. Fig. 10 shows that as we are increasing the mass, keeping velocity and all other parameters constant, penetration depth increases. This is an expected trend. However, this should be kept in mind that practically it is not always feasible to increase the mass dramatically without affecting its velocity. Keeping this in view, this parametric study has been conducted for a small variation in mass (22 to 24 kg). An increase of 10 % in the mass results in 5 % increase in the penetration depth.

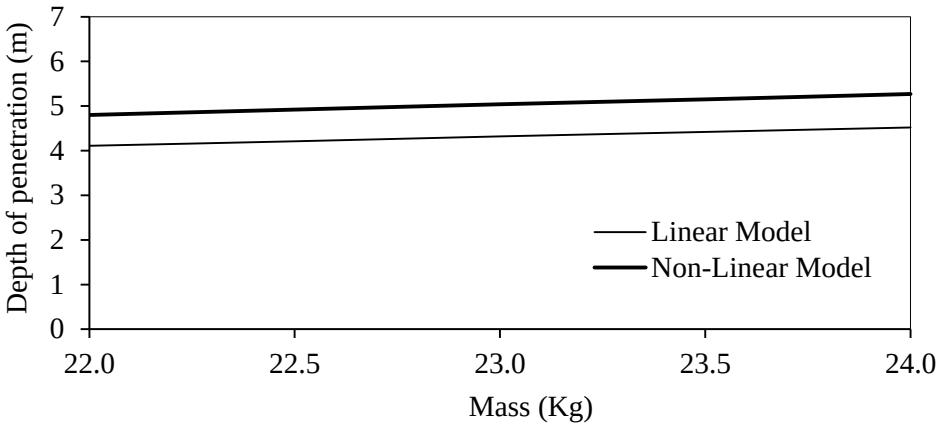

Fig. 10 Effect of mass on penetration depth

6.4.4. Effect of modulus of elasticity

The modulus of elasticity is not a simple parameter to obtain for any soil; its value varies with the soil type, state of compaction/consolidation, quantity of moisture, confinement and depth. Therefore, there may be a large variation in its estimation. It was observed that as the modulus of elasticity of soil increases, it makes the soil stiffer which consequently makes the missile penetration difficult into the soil. It is due to this reason, increase in maximum deceleration, decrease in depth of penetration and decrease in stopping time (Table 7). It is observed for present study model that an increase of 30 % in the value

of Young's modulus (E), the reduction in the penetration depth of 3.2 % and 2.4 % for linear and non-linear model. The predicted values of penetration depth by present study linear and non-linear models are 19 % and 6 % respectively less than the experiment value (Fig. 11).

Table 7 Influence of variation in value of Young's modulus (E)

Value of E (MPa)	Maximum deceleration (g)		Minimum deceleration (g)		Final time t_f (ms)	Penetration depth (m)		Penetration depth (m)	
	Linear	Non-linear	Linear	Non-linear	Linear	Non-linear	Linear	Non-linear	Experiment
120	3746	2841	799	713	34.0	39.0	4.57	5.26	-
160	3763	2979	842	741	32.5	37.5	4.34	5.08	5.04
210	3775	2761	878	763	31.0	36.5	4.17	4.95	-

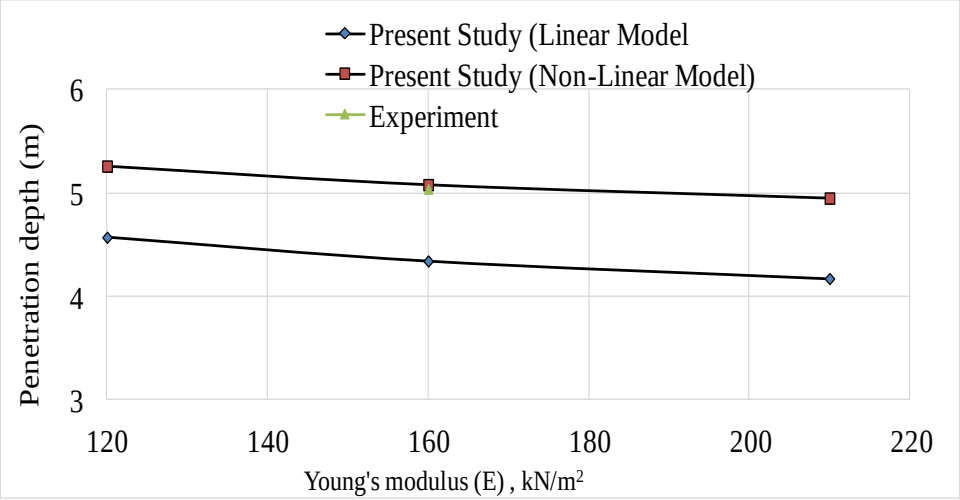

Fig. 11 Effect of modulus of elasticity on penetration depth

7. Concluding Remarks

Forrestal and Luk model gave the predicted penetration depth less than the experimental values obtained in this study because he considered the drag force maximum at tip of nose which remains constant along nose length. But in present model study, the forces are taken minimum at tip, increasing along length of nose and become maximum at end of nose and then remain constant throughout the length of shaft of projectile. The present experimental and values predicted in proposed model has provided a significant improvement in the Forrestal and Luk model. The predicted penetration depths by the proposed model are less than the experimental results in dry, saturated and compacted sand.

The observations made from the experiments are as follows:

i) As expected, the depth of penetration reduces with the increase in nose angle or reduction in the nose length of ogival nose projectiles in all types of soil targets.

ii) The penetration depth of projectiles was more in saturated sand than compacted sand. The reason for this trend is that the angle of shearing resistance of saturated sand reduces about 50%, thus reducing the friction between sand particles and projectile nose.

iii) There is significant influence of *CRH* on penetration depth. The penetration depth increases with the increase in the value of *CRH* as shape of the missile nose becomes more pointed that makes the penetration easier. The missile of same CRH in the non-linear material stops at greater depth than the linear soil material.

iv) A decrease of 10 % in value of coefficient of friction results in an increase in penetration depth by 6.5 % for both linear and non-linear models. For the same coefficient of friction, nonlinear model offers lesser resistance, thus results in greater penetration depth.

v) An increase of 10 % in the mass of projectile results in 5 % increase in penetration depth.

vi) Increase in the modulus of elasticity of soil cause increase in maximum deceleration, decrease in depth of penetration and decrease in stopping time.

The results obtained from present experimental study can be used in making the strategic underground structures safe against enemy projectile attack by either constructing the structure at a safe depth or if such placement is not economically feasible then the structure may be designed to resist the forces exerted by the projectile.

References

[1] Abbas H, Paul DK, Godbole PN, Nayak GC. Soft projectile impact on rigid target, International Journal of Impact Engineering, 1995, Nos. 5-6, Vol. 16, pp. 727-37.

[2] Allen WA. Dynamics of projectile penetrating sand, Journal of Applied Physics, 1957, Vol. 28.

[3] Boguslavskii Yu, Drabkin S, Salman A. Analysis of vertical projectile penetration in granular soils, Journal of Physics, D: Applied Physics, 1996, No. 3, Vol. 29, pp. 905-916.

[4] Corbett CG, Reid SR, Johnson W. Impact loading of plates and shells by free flying projectiles: a review, International Journal of Impact Engineering, 1996, pp. 141-230.

[5] Danziger BR, Costa AM, Lopes FR, Pacheco MP. Back analysis of offshore pile driving with an improved soil model, geotechnique, The Institution of Civil Engineers, London, 1999, No. 6, Vol. 49.

[6] Euler L. Neue Grunds atze der Artillerie, Berlin (Reprinted Euler's Opera Omnia Vol. 14, Series II (Teubner), 1745.

[7] Forrestal MJ, Longscope DB, Norwood FR. A model to estimate forces on conical penetrates into dry porous rock, Journal of Applied Mechanics, ASME, 1981, Vol. 48, pp. 25-29.

[8] Forrestal MJ, Lee LM, Jenrette LM. Laboratory-scale penetration experiments into geological targets to impact velocities of 2.1 km/s, ASME Journal of Applied Mechanics, 1986, Vol. 53, pp. 317-320.

[9] Forrestal MJ, Luk VK. Penetration into Soil Targets, International Journal of Impact Engineering, 1992, No. 3, Vol. 12, pp. 427-444.

[10] Forrestal MJ, Hanchak SJ. Penetration limits velocity for ogive nose projectiles and limestone targets, ASME Journal of Applied Mechanics, 2002, Vol. 69, pp. 853-854.

[11] Hearst JR, Lynch CS. Measurement of in-situ strength using projectile penetration, International Journal of Rock Mechanics, Mining Science Geomechanics, 1994, Vol. 31, pp. 243-251.

[12] Norwood FR, Sears MP. A nonlinear model for the dynamics of penetration into geological targets, Transactions of ASCE, 1982, Vol. 49, pp. 26-30.

[13] Robins B. New Principles of Gunnery, London, 1742.

[14] Seguin, A, Bertho Y, Gondret P. Penetration of a Projectile by Impact into a Granular Medium, Traffic and Granular Flow, 2009, Vol. 7, pp. 647-652.

[15] Taylor T, Fragaszy RJ, Ho CL. Projectile penetration in granular soils, Journal of Geotechnical Engineering, 1991, No. 4, Vol. 117, pp. 658-672.

[16] Thompson JB. Low-Velocity Impact Penetration of Low-Cohesion Soil Deposits, Dissertation for the Degree of Doctor of Philosophy in Engineering University of California, Berkeley, 1975.

[17] Yankelevsky DZ. Analysis of impact and penetration to geomaterials using engineering models, Journal of Applied Mechanics, ASME, 1988, pp. 67-81.

[18] Yu HS, Mictchell JK. Analysis of cone resistance: review of methods, Journal of Geotechnical and Geo-environmental Engineering, ASCE, 1998, No. 2, Vol. 124, pp. 140-149.

[19] Zukas JA, Nicholas T, Swift HF, Greszczuk LB, Curran DR. Impact Dynamics, John Wiley & Sons, Inc, USA, 1982.